Ind. J. Pharm. Edu. Res., 2025; 59(2):757-766.
https://www.ijper.org

Original Article

Chlorogenic Acid Functionalized Tin Oxide-Sodium Alginate Hybrid Nanomaterials Induce Oxidative Stress-Mediated Apoptosis in Breast Cancer MDA-MB-231 Cells

Baby Shakila[1], Nouf M. Alyami[2], Hossam M. Aljawdah[2], Sulaiman Ali Alharbi[3], Palanisamy Arulselvan[4], Saravana Kumar Jaganathan[5], Samer Hasan Hussein Al Ali[6], Muruganantham Bharathi[7,*]

[1]Department of Biochemistry, Vivekanandha College of Arts and Sciences for Women (Autonomous), Elayampalayam, Tiruchengode, Namakkal, Tamil Nadu, INDIA.
[2]Department of Zoology, College of Science, King Saud University, Riyadh, SAUDI ARABIA.
[3]Department of Botany and Microbiology, College of Science, King Saud University, Riyadh, SAUDI ARABIA.
[4]Department of Chemistry, Saveetha School of Engineering, Saveetha Institute of Medical and Technical Sciences (SIMATS), Saveetha University, Chennai, Tamil Nadu, INDIA.
[5]School of Engineering and Physical Sciences, University of Lincoln, UNITED KINGDOM.
[6]Department of Chemistry, Faculty of Sciences, Isra University, Amman, JORDAN.
[7]Department of Biochemistry, Centre for Bioinformatics, Karpagam Academy of Higher Education, Coimbatore, Tamil Nadu, INDIA.

ABSTRACT

Background: Nanotechnology has emerged as a novel research area to address the several problems associated with existing cancer treatments. **Objectives:** The present work was focused on synthesizing and characterizing the tin oxide-sodium alginate-chlorogenic acid hybrid nanomaterials (SnO_2-SA-CA HNMs) for enhanced anticancer effects against breast cancer MDA-MB-231 cells. **Materials and Methods:** The synthesized SnO_2-SA-CA HNMs were characterized using several methods, including UV-vis spectroscopy, X-ray Diffraction (XRD), Scanning Electron Microscopy (SEM), Transmission Electron Microscopy (TEM), Energy Dispersive X-ray (EDX), Fourier Transform Infrared (FT-IR), Dynamic Light Scattering (DLS) and Photoluminescence (PL) analyses. The MTT assay was done to assess the cytotoxicity of SnO_2-SA-CA HNMs against MDA-MB-231 cells. The apoptotic cell death was analyzed by the dual staining assay. The oxidative stress parameter levels were analyzed using corresponding assay kits. **Results:** The results of the different characterization studies are confirmed the formation of metallic SnO_2-SA-CA HNMs with an average size of 93 nm. The SnO_2-SA-CA HNMs have a crystalline nature, clustered morphology and cuboidal structures. The existence of various functional groups and elements in the HNMs was also confirmed by the FT-IR and DLS analyses, respectively. The SnO_2-SA-CA HNMs have demonstrated a substantial effect on inhibiting the viability of MDA-MB-231 cells. The dual staining result also proved the onset of apoptotic cell death in the HNMs-treated cells. The HNMs treatment effectively decreased the antioxidant level, thereby promoting oxidative stress. **Conclusion:** The present findings suggest that SnO_2-SA-CA HNMs exhibit potential as a potential therapeutic candidate to treat breast cancer.

Keywords: Breast cancer, Nanomaterials, Apoptosis, Oxidative stress, Chlorogenic acid.

Correspondence:
Dr. Muruganantham Bharathi
Department of Biochemistry, Centre for Bioinformatics, Karpagam Academy of Higher Education, Coimbatore-641021, Tamil Nadu, INDIA.
Email: bharathi.m@kahedu.edu.in

Received: 27-05-2024;
Revised: 13-07-2024;
Accepted: 06-12-2024.

INTRODUCTION

The field of nanomedicine has progressed as a new scientific discipline in the pursuit of modern personalized medicine. It uses Nanoparticles (NPs) for the purposes of disease diagnosis, imaging, diagnosis and treatment. NPs within the size range of 10-100 nm are often considered to be highly beneficial for drug delivery purposes.[1] The NPs demonstrate exceptional mobility within the human body, enabling easy movement between organs and effective infiltration into targeted regions.[2] NPs have the potential to bind with drugs, which helps in specifically targeting affected tissues. NPs are characterized by their significantly smaller dimensions in comparison to blood cells and they have a size that is nearly equivalent to that of DNA. This enables the improvement of their activity and provides them with unique physical, chemical and optical characteristics that make them acceptable for use in medicines for cancer treatment

DOI: 10.5530/ijper.20257391

and diagnosis. Furthermore, they have the capacity to enhance traditional treatment methods.[3]

Cancer has historically posed a significant and widespread threat, resulting in a substantial impact on both global health and the economy. Cancer cells possess the ability to elude the immune system, replicate continuously and initiate angiogenesis, resulting in formidable malignancies that directly risk human life.[4] Breast cancer is a common type of cancer among women worldwide and is classified as a malignant tumor that arises in the breast tissues. The GLOBOCAN 2020 report indicates that there have been 2.3 million incidences of breast cancer reported worldwide, responsible for 11.7% of all cancer incidences.[5,6] Genetic, hormonal, environmental and dietary changes determine the etiology of breast cancer.[7] The risk factors encompass the history of breast cancer, a familial predisposition to the disease, being obese, excessive tobacco use, excessive alcohol use, a physically inactive lifestyle and the use of hormone replacement treatment. Around 80% of individuals diagnosed with breast cancer are aged 50 or older and the likelihood of developing the disease increases with age.[8]

Chemotherapy is the predominant therapeutic strategy for treating cancer. Depending on the stage of cancer, chemotherapy can achieve successful results when used alone or in combination with other methods like radiotherapy, surgery, or adjuvant therapies.[9] Nevertheless, the inadequate specificity, poor solubility in an aqueous environment and short circulation period in the bloodstream of traditional anticancer drugs result in low levels of pharmaceuticals reaching the tumor location and necessitate the use of high doses. Furthermore, the effectiveness of drugs decreases with time as a result of the emergence of drug resistance. Although there has been an increase in the development of anticancer medicines in recent decades, their significant toxicity, expensive production and limited patient adherence necessitate the search for more effective antitumor alternatives.[10]

Nanotechnology has emerged as a novel research area to address the several problems associated with existing cancer treatments.[11-13] Alginates are naturally occurring polysaccharides with polyanionic properties. Alginates are derived from marine brown algae and bacteria. Alginate-based nanomaterials are becoming increasingly popular in the fields of drug/gene delivery.[14] Alginates, when combined with biomaterials, provide appealing nanostructures and enable the precise and regulated release of therapeutic drugs to combat cancers. Various novel formulations with anticancer properties can utilize alginates as a base material.[15]

Tin oxide (SnO_2) NPs are n-type semiconductors and possess a broad band gap of 3.6 eV. SnO_2 NPs are highly suitable as photocatalysts because of their potent oxidizing capacity, morphology, lack of toxicity and exceptional resistance to photochemical degradation.[16,17] Chlorogenic Acid (CA) is a major bioactive compound mostly found in many plants, such as coffee beans, apples and tea. CA has demonstrated significant potential as a phenolic acid, making it a valuable candidate for use as a nutraceutical. Several studies have well reported the effectiveness of CA in reducing oxidative stress, mitigating inflammation and addressing problems related to glucose and lipid metabolism.[18-20] Several studies have already highlighted the potential anticancer properties of CA.[21-23] A recent report indicated the therapeutic effects of CA-conjugated NPs in suppressing tumors.[24] The present study was aimed at synthesizing and characterizing the tin oxide-Sodium Alginate-CA Hybrid Nanomaterials (SnO_2-SA-CA HNMs) for enhanced anticancer activity against breast cancer MDA-MB-231 cells.

MATERIALS AND METHODS

Chemicals

Chlorogenic acid, Sodium Alginate (SA), tin chloride and other major chemicals and reagents were purchased from Sigma-Aldrich, USA. The ELISA assay kits to quantify the oxidative stress parameters were obtained from ElabScience, USA.

Synthesis of the SnO_2-SA-CA HNMs

The chemical precipitation technique was employed to synthesize the SnO_2-SA-CA HNMs. Tin chloride (0.1 M) and 500 mg of SA were dissolved in 50 mL of an aqueous solution. In addition, 50 mg of chlorogenic acid was added to the SnO_2-SA solution. About 0.1 M of NaOH solution was added to the SnO_2-SA-CA solution. A white residue has been obtained, which was heated for 3 hr using the magnetic stirrer. The obtained residue was then rinsed with deionized water and an ethanol solution. The resulting suspension was then centrifuged for 40 min at -3°C at 15,000 rpm and the resulting product was dehydrated at 200°C for 2 hr.

Characterization of the SnO_2-SA-CA HNMs

The UV-Visible spectrophotometer (Shimadzu-1700, Tokyo, Japan) was employed to measure the UV-visible absorbance spectrum of the SnO_2-SA-CA HNMs at wavelengths ranging from 200-1000 nm. The Photoluminescence (PL) analysis of the SnO_2-SA-CA HNMs was conducted using the spectrofluorimeter (F-2500 FL, Hitachi) to assess the optoelectric properties of the HNMs. The X-ray Diffraction (XRD) patterns of the SnO_2-SA-CA HNMs were obtained using an XRD Panalytical X-pert Pro instrument (PANanalytical, Netherlands) operating at 30 kV and 30 mA. The scanning rate was set to 2°/min and the spectrum was taken at the 10-80° range of 2 Θ angles. The SnO_2-SA-CA HNMs were subjected to Dynamic Light Scattering (DLS) analysis using a DLS machine (HORIBA, Kyoto, Japan) to determine their distribution patterns and average particle size. The surface morphology and size of the SnO_2-SA-CA HNMs were studied

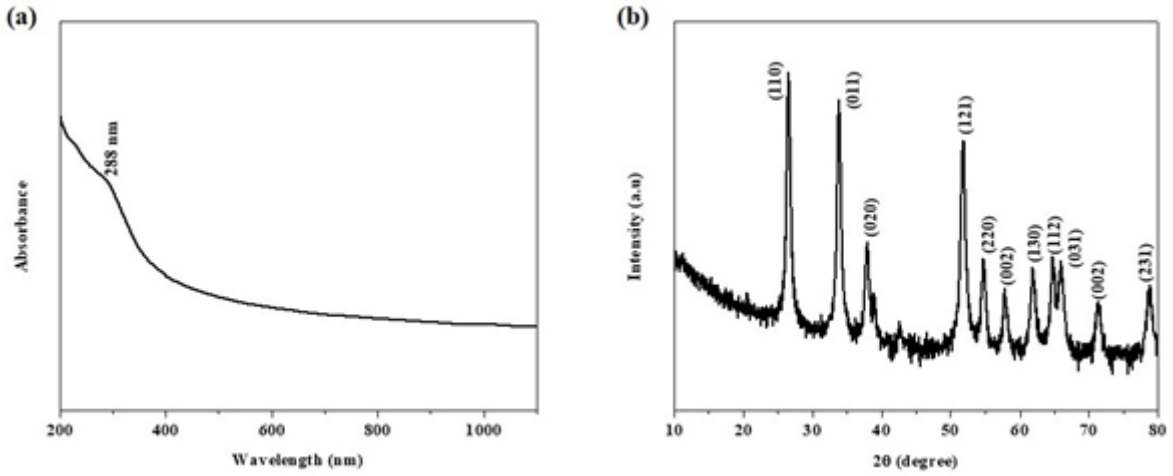

Figure 1: UV-vis spectroscopy and XRD analyses of the SnO_2-SA-CA HNMs. The analysis of absorbance at various wavelengths (200-1000 nm) demonstrated the highest peak at 388 nm, suggesting the formation of SnO_2-SA-CA HNMs (a). The XRD analysis represented the precise crystallographic orientations of the SnO_2-SA-CA HNMs in their crystalline nature (b).

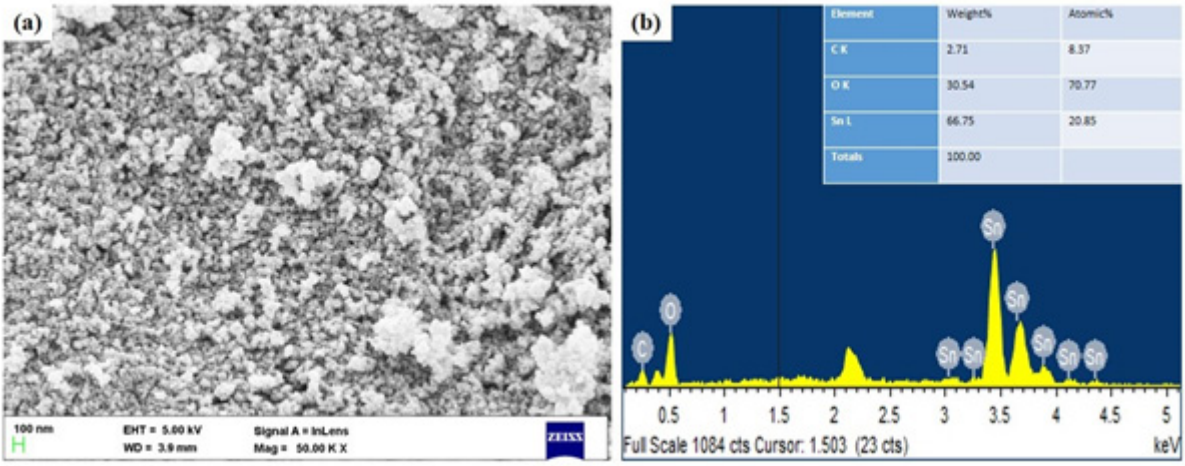

Figure 2: SEM and EDX analyses of the SnO_2-SA-CA HNMs. The SEM microphotographs showed that the SnO_2-SA-CA HNMs displayed a circular shape with a clustered morphological appearance (a). EDX analysis of the SnO_2-SA-CA HNMs revealed clear peaks, indicating the presence of various elements, including C, O and Sn (b).

using a scanning electron microscope (SEM; TM3000, Hitachi, Japan). The SnO_2-SA-CA HNMs were analyzed using an Energy Dispersive X-ray analysis (EDX) spectrometer to determine their elemental profiles. The SnO_2-SA-CA HNMs were analyzed using a JEOL-JEM T1010 Transmission Electron Microscopy (TEM) to measure their morphology and approximate particle sizes. The surface functional groups of the SnO_2-SA-CA HNMs were studied using Fourier Transform Infrared spectroscopy (FTIR; VERTEX 70 model, Bruker, Germany).

In vitro assays

Cell line collection and maintenance

The MDA-MB-231 breast cancer cells were obtained from the ATCC, USA. Afterwards, the cells were grown in a CO_2 incubator at 37°C, using DMEM medium with 10% FBS and 1% antimycotic combinations. After achieving 80% confluency, cells were treated with trypsin, separated and used for additional experiments.

MTT assay

The MTT assay was performed to evaluate the viability of both untreated and HNMs-treated cells. The cells were cultivated in 96-well plates at 5×10^3 cells/well population for 24 hr. Following a 24 hr incubation period, the cells were treated with different dosages (2.5, 5, 10, 15, 20, 25 and 30 µg/mL) of the SnO_2-SA-CA HNMs for 24, 48 and 72 hr. Each well was then mixed with MTT reagent (20 µL) and DMEM (100 µL) and incubated for 4 hr. The formazan precipitates that were developed in wells were then dissolved using 100 µL of DMSO and the absorbance was taken at 570 nm.

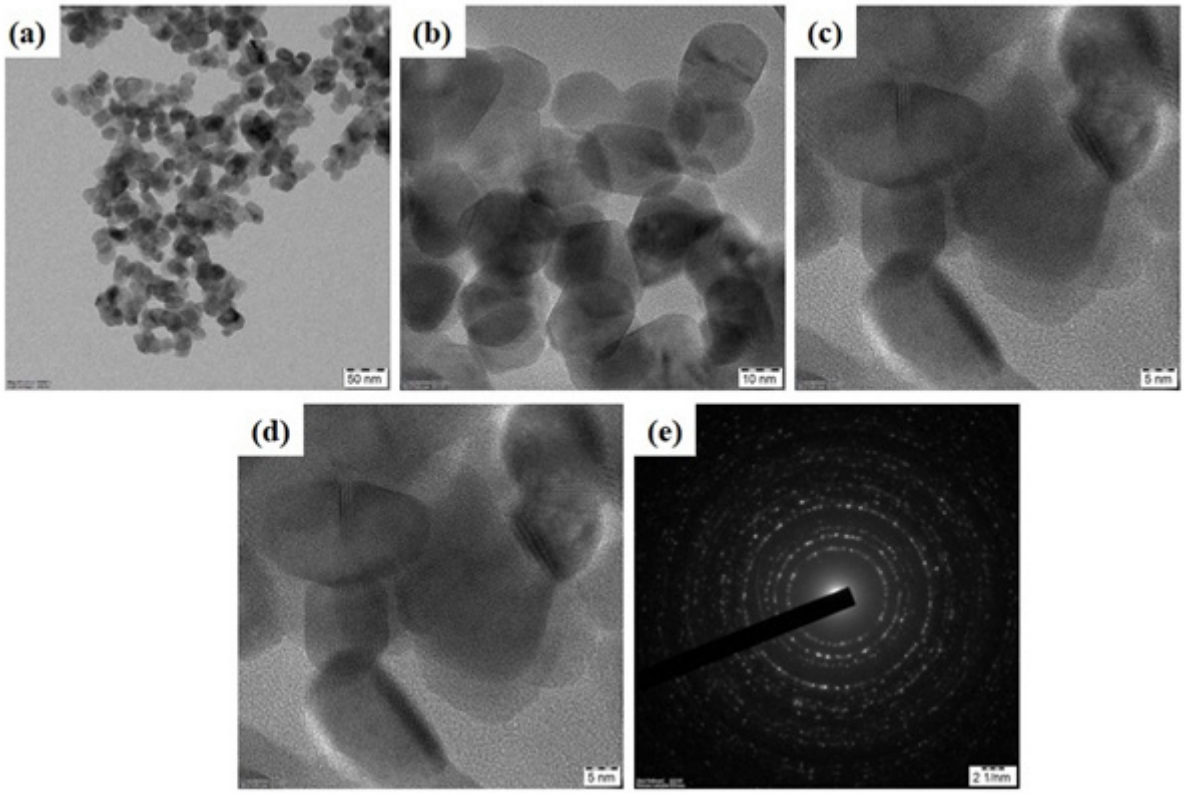

Figure 3: TEM analysis of the SnO_2-SA-CA HNMs. The TEM microphotographs showed that the synthesized SnO_2-SA-CA HNMs displayed cuboid-like shapes (a-d). Analyzing the SAED patterns confirmed the crystallization of the SnO_2-SA-CA HNMs (e).

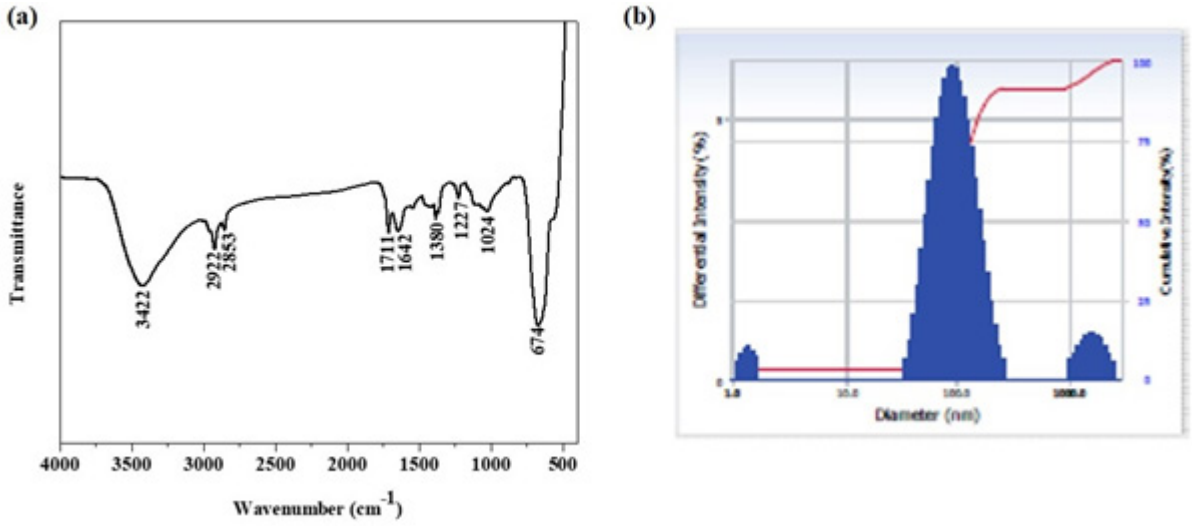

Figure 4: FTIR and DLS analyses of the SnO_2-SA-CA HNMs. The synthesized SnO_2-SA-CA HNMs displayed several peaks dispersed across multiple frequencies, which confirms the presence of various functional groups (a). The results of the DLS analysis indicated a less scattered distribution with an average particle size of 93 nm (b).

Dual staining

The apoptosis in both untreated and HNMs-treated cells were studied using the dual staining technique. The cells were cultivated on a 24-well plate and treated with 15 and 20 µg/mL of the SnO_2-SA-CA HNMs for 24 hr. After wards, the cells underwent a staining procedure utilizing an AO/EtBr dye mixture at 100 µg/mL in a 1:1 proportion for 5 min. After the staining procedure, the fluorescence level was evaluated using a fluorescent microscope.

Analysis of oxidative stress markers

Assay kits were used to analyze the levels of Malondialdehyde (MDA), Glutathione (GSH), Superoxide Dismutase (SOD) and Catalase (CAT) in the cell lysates of untreated and SnO_2-SA-CA

HNMs-treated MDA-MB-231 cells. The assays were conducted in accordance with the recommended protocols of the manufacturer (ElabScience, USA).

Statistical analysis

The data set was statistically analyzed using SPSS software and the final results are depicted as a mean±SD of triplicates (n=3). The data were examined using one-way ANOVA and Dunnett's multiple range test to analyze the significance (p<0.05) between values.

RESULTS

Characterization results of the SnO_2-SA-CA HNMs

Figure 1(a) displays the findings of the UV-visible spectroscopy on the SnO_2-SA-CA HNMs. The analysis of absorbance at various wavelengths (200-1000 nm) demonstrated a significant peak at 388 nm, suggesting the formation of SnO_2-SA-CA HNMs. The XRD analysis was used to evaluate the purity and crystalline characteristics of the SnO_2-SA-CA HNMs (Figure 1b). The peaks shown in Figure 1(b), such as 110), (101), (200), (111), (211), (220), (102), (301), (202) and (321) hkl planes of SnO_2-SA-CA HNMs, which are generally matched with the tetragonal rutile-type SnO_2 (space group P42/mnm) crystalline structure (JCPDS No. 41-1445). of the SnO_2-SA-CA HNMs in their crystalline form.

The morphology and elemental composition of the synthesized SnO_2-SA-CA HNMs were evaluated using SEM and EDX analyses, respectively. The SEM microphotographs (Figure 2a) showed that the SnO_2-SA-CA HNMs exhibits a spherical structure. EDX examination of the SnO_2-SA-CA HNMs revealed clear peaks, indicating the presence of various elements, including C, O and Sn (Figure 2b). Figure 3(a-d) displays the microphotographs of the synthesized SnO_2-SA-CA HNMs, which were taken by TEM analysis. The TEM microphotographs showed that the synthesized SnO_2-SA-CA HNMs displayed spherical structure, with an average diameter of 72 nm. Analyzing the SAED patterns (Figure 3e) confirmed the crystallization of the SnO_2-SA-CA HNMs.

The FT-IR analysis was performed to determine the surface functional groups bound on the synthesized SnO_2-SA-CA HNMs (Figure 4a). The synthesized SnO_2-SA-CA HNMs displayed several peaks dispersed across multiple frequencies. The prominent peak at 3422 cm-1 can be attributed to the vibrational band due to the stretching movement of the O-H bond. The C-H asymmetric and symmetric stretching is shown by peaks detected at wavenumbers of 2922 cm^{-1} and 2853 cm^{-1}. The peaks observed at wavenumbers of 1711 cm^{-1}, 1642 cm^{-1}, 1380 cm^{-1} and 1227 cm^{-1} can be attributed to the bending vibrations of C=O, O-H, C-H and C-O bonds. The peaks detected at 1024 cm^{-1} and 674 cm^{-1} are indicative of the existence of H-O and O-Sn-O bonds. Figure 4(b) illustrates the findings of DLS analysis, which show the dispersion and particle size of the synthesized SnO_2-SA-CA HNMs. The DLS results indicated a less scattered distribution with an average particle size of 93 nm.

The findings of a PL analysis of the SnO_2-SA-CA HNMs are shown in Figure 5. The specific wavelengths at which the excitations of the SnO_2-SA-CA HNMs were noted were 367, 396, 399, 415, 436, 457 and 480 nm, respectively. The PL spectrum reveals details about the crystal structure, surface properties and structural imperfections shown by the SnO_2-SA-CA HNMs. The presence of peaks at a wavelength of 367, 396 and 399 nm indicates the transition from the shallow donor level formed by oxygen vacancies V_O^{o}. The violet emission observed at 415 nm, is due to an electron moving from the conduction band to the acceptor level caused by V_O^{++} being just above VB. The blue emission observed at 436, 457 and 480 nm, which is corresponding to the transition from the donor level formed by V_O^{+} to the valence band and electron transition from oxygen vacancies V_O^{o} to doubly ionized oxygen vacancy V_O^{++}, as shown in Figure 5.

SnO_2-SA-CA HNMs inhibit the viability of MDA-MB-231 cells

The cytotoxicity of SnO_2-SA-CA HNMs on the viability of MDA-MB-231 cells was examined by MTT assay and the findings are demonstrated in Figure 6. The MTT assay results demonstrate that the treatment of SnO_2-SA-CA HNMs at diverse dosages (2.5, 5, 10, 15, 20, 25 and 30 µg/mL) significantly reduced the viability of cells. A drastic reduce in the viability was noted upon treatment with increased concentrations of SnO_2-SA-CA HNMs. The IC_{50} value of the SnO_2-SA-CA HNMs was noted to be 15 µg/mL for 48 hr treatment. Therefore, dosages of 15 and 20 µg/mL were used for the subsequent experiments as IC_{50} and high doses, respectively.

SnO_2-SA-CA HNMs induce apoptosis in MDA-MB-231 cells

The findings of the dual staining assay are shown in Figure 7, which confirms the apoptotic properties of SnO_2-SA-CA HNMs. The assay findings demonstrate that the treatment with SnO_2-SA-CA HNMs at different concentrations (15 and 20 µg/mL) led to a higher number of yellow and orange fluoresced cells compared to the untreated cells. The green fluorescent cells in the control show the presence of normal viable cells, whereas the increased number of yellow and orange fluorescent cells in the SnO_2-SA-CA HNMs-treated cells suggests the occurrence of more early and late apoptosis, respectively (Figure).

SnO_2-SA-CA HNMs induce oxidative stress in MDA-MB-231 cells

Figure 8 illustrates the effect of SnO_2-SA-CA HNMs treatment on the levels of MDA and antioxidants (GSH, CAT and SOD) in the MDA-MB-231 cells. The treatment of cells with SnO_2-SA-CA HNMs leads to a remarkable elevation in MDA levels. In addition, the SnO_2-SA-CA HNMs treatment significantly

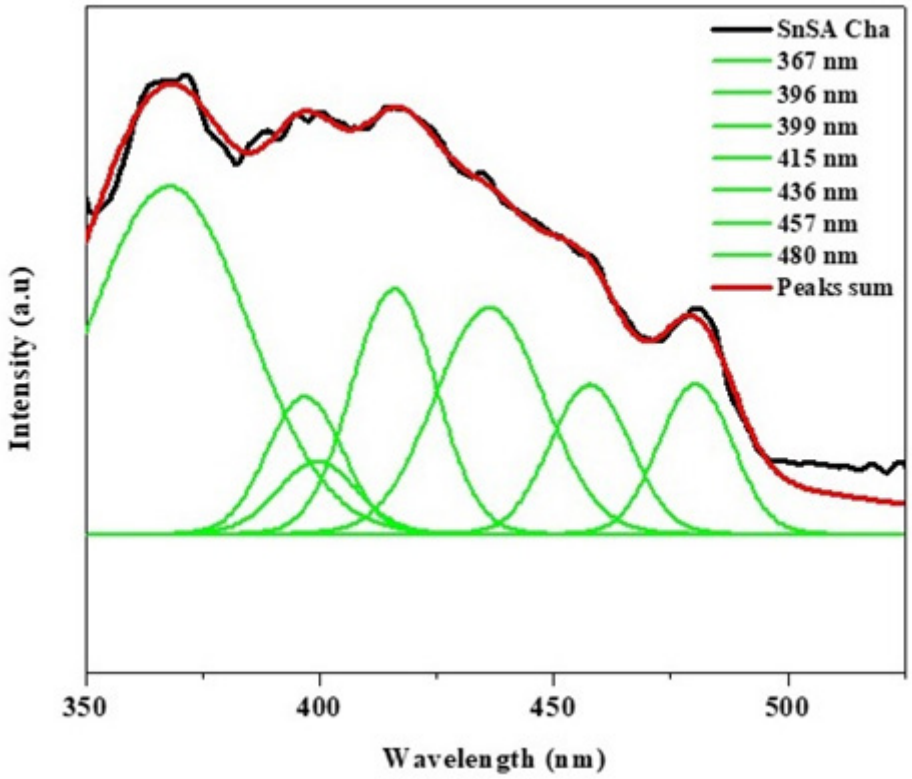

Figure 5: PL spectroscopic analysis of the SnO_2-SA-CA HNMs. The specific wavelengths at which the excitations of the SnO_2-SA-CA HNMs were noted were 367, 396, 399, 415, 436, 457 and 480 nm, respectively. The PL spectrum reveals details about the crystal structure, surface properties and structural imperfections shown by the SnO_2-SA-CA HNMs.

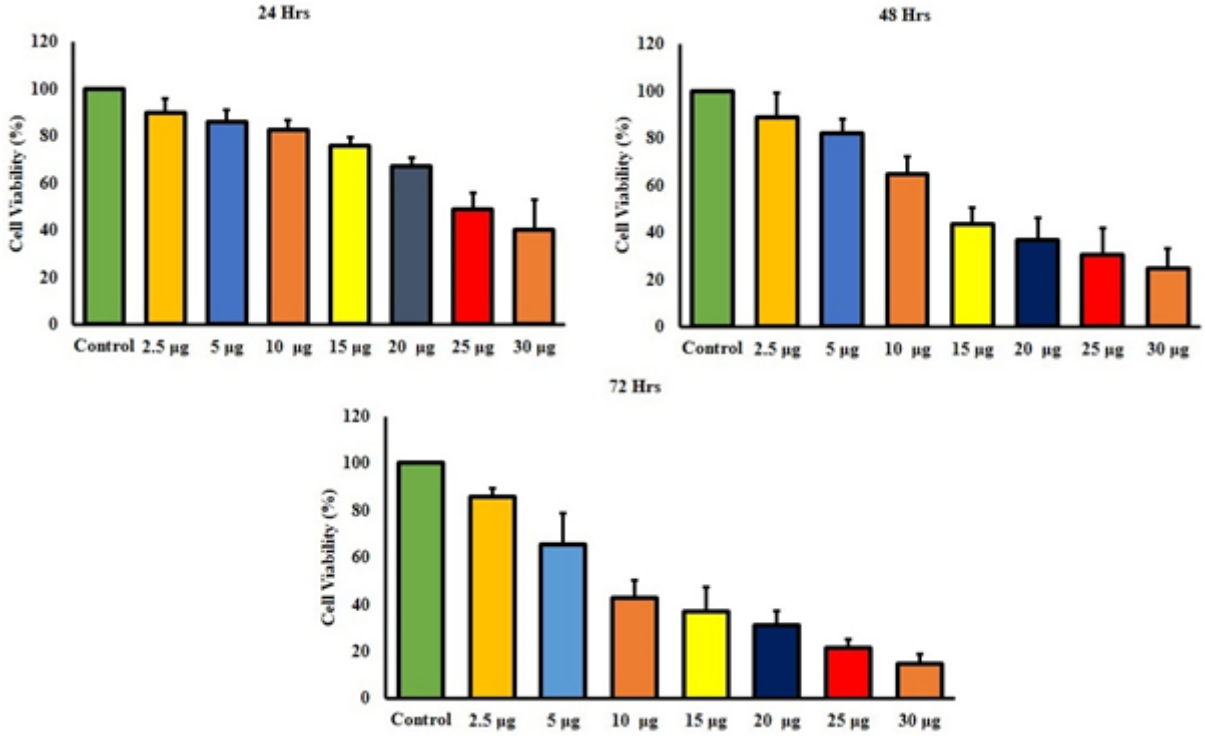

Figure 6: Effect of SnO_2-SA-CA HNMs on the viability of breast cancer MDA-MB-231 cells. The data were statistically analyzed using SPSS software and the final results are depicted as the mean±SD of triplicate measurements (*n*=3). The data were examined using a one-way ANOVA and Dunnett's multiple range tests to determine the significance level.

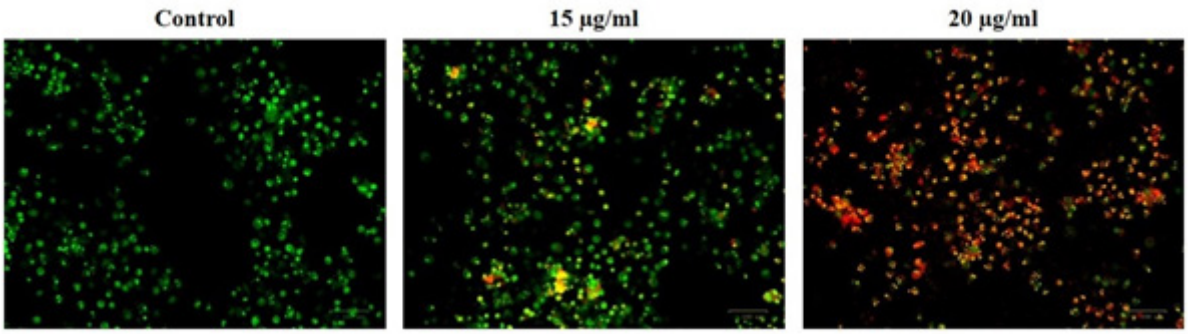

Figure 7: Effect of SnO_2-SA-CA HNMs on the apoptotic cell death in the MDA-MB-231 cells. The green fluorescent cells in the control group show the presence of normal viable cells, whereas the increased number of yellow and red fluorescent cells in the SnO_2-SA-CA HNMs-treated cells suggests the presence of more early and late apoptotic cells, respectively.

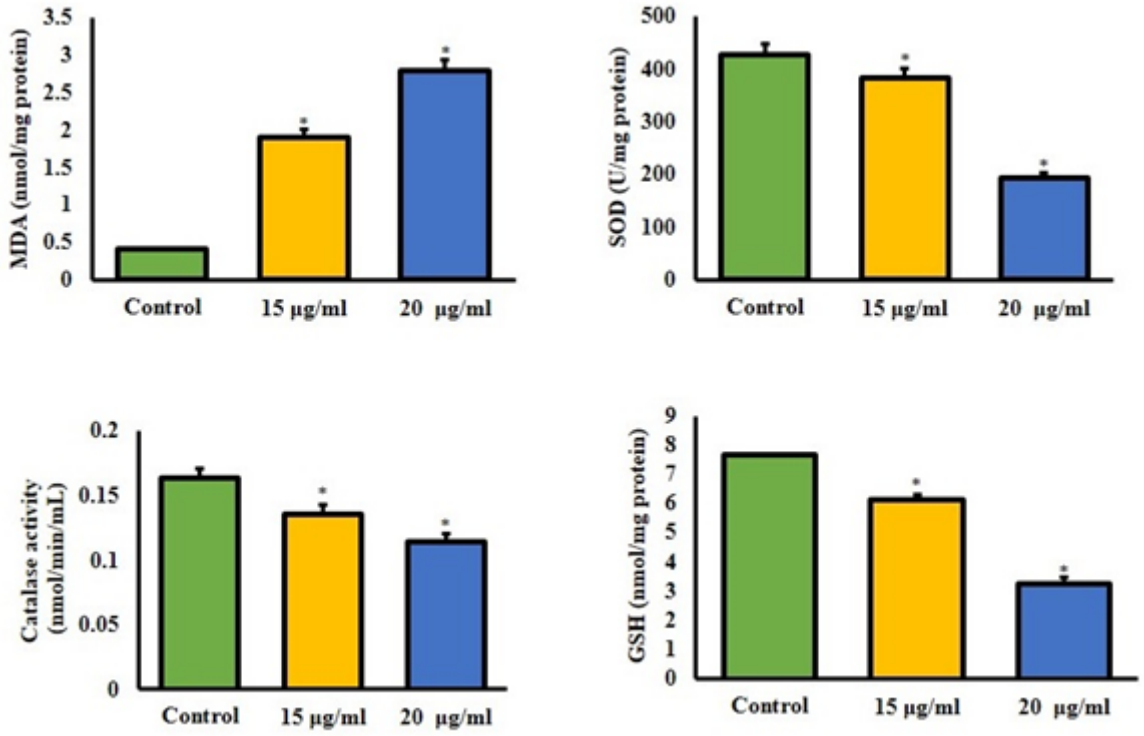

Figure 8: Effect of SnO_2-SA-CA HNMs on the oxidative stress biomarkers MDA, GSH, CAT and SOD in the MDA-MB-231 cells. The data were statistically analyzed using SPSS software and the final results are depicted as the mean±SD of triplicate measurements (n=3). The data were examined using a one-way ANOVA and Dunnett's multiple range tests to determine the significance level. '*' indicates that the values significantly differ at $p<0.05$ from the control.

decreased the GSH, CAT and SOD levels in the MDA-MB-231 cells. The findings of this assay showed a notable reduction in antioxidant levels and a simultaneous increase in oxidative stress in SnO_2-SA-CA HNMs-treated MDA-MB-231 cells (Figure 8).

DISCUSSION

Recently, the advantageous physical, chemical and biological characteristics of natural materials have made them highly attractive as base materials for cancer therapy. Additionally, they possess functional groups that enable easy chemical modification for the development of even more effective formulations.[25] Furthermore, comprehensive toxicology evaluations are essential for the successful application of nanoparticulate and nanomedicines in clinical settings. The advantageous biological characteristics of natural NPs may offer a potential advantage in terms of expedited integration into clinical trials and subsequent adoption in medical practice in comparison to synthetic alternatives.[26]

Chemotherapy, surgical excision of the malignant tissue, radiotherapy, immunotherapy and a combination of these treatments has traditionally been employed to treat cancers. Despite challenges such as systemic toxicity, low selectivity many undesirable effects and traditional chemotherapeutics

remain the primary method to treat advanced tumors. Cancer treatment often uses drugs that selectively target rapidly dividing cells, resulting in unwanted adverse effects on healthy cells.[27] The standard hormone and chemotherapeutic drugs have inadequate therapeutic effects and unsatisfactory pharmacokinetic responses, as well as a lack of specificity.[28] In order to address these problems, nanomedicines have gained increased interest due to their ability to deliver drugs effectively while optimizing pharmacokinetics and pharmacodynamics. Nanomedicine refers to the use of NPs to tackle healthcare issues.[29] Therefore, this work aimed to study the anticancer properties of the synthesized SnO_2-SA-CA HNMs against breast cancer MDA-MB-231 cells.

The characterization of NPs mainly relies on the study of particle size (or diameter) and surface area attributes. Electron microscopy techniques, such as SEM and TEM, can accurately measure the surface morphology, size and shape of the NPs. DLS is a frequently employed technique for determining the dimensions of NPs. The hydrodynamic diameter, as studied by DLS, specifically denotes the diffusion behavior of a particle in a fluid environment. In this study, the results of the different characterization studies confirm the formation of metallic SnO_2-SA-CA HNMs with an average size of 93 nm. The SnO_2-SA-CA HNMs have a crystalline form, clustered morphology and cuboidal structures. The FT-IR and DLS analyses confirmed the occurrence of various functional groups and elemental profiles in the SnO_2-SA-CA HNMs, respectively.

Nanotechnology has been extensively studied and employed in the area of cancer therapy.[30] It also facilitates lower doses of the drug to be used while still achieving the desired therapeutic effect. In recent times, NPs have gained significant attention in the biomedical domain, particularly in drug delivery.[31,32] Most of the anticancer drugs exert their activity by either inhibiting or eradicating the growth of cancer cells.[33] In this study, the findings clearly demonstrated that the synthesized SnO_2-SA-CA HNMs effectively inhibited the viability of MDA-MB-231 cells, which supports the cytotoxic properties of the SnO_2-SA-CA HNMs against breast cancer cells.

Apoptosis plays a pivotal role in regulating cellular homeostasis and preventing cancer growth. Apoptosis is characterized by nuclear fragmentation, cell shrinkage, the degradation of RNA and the fragmentation of DNA. The nucleus shows the structural changes of apoptosis, such as chromatin condensation and nuclear disintegration. During apoptosis, cells develop apoptotic bodies that contain a specific phospholipid called phosphatidylserine. Phosphatidylserine efficiently functions as a signaling molecule, notifying neighboring cells, which is identified as an early apoptotic mechanism. Late apoptosis is an irreversible condition characterized by complete cytoskeleton disaggregation, cell permeation and disintegration.[34-37] Therefore, developing innovative therapeutic strategies that selectively target the apoptotic process in cancer treatment has great promise. In the MDA-MB-231 cells treated with SnO_2-SA-CA HNMs, the dual staining assay showed that there were both early and late stages of apoptotic cell death. Therefore, it was clear that the SnO_2-SA-CA HNMs can induce apoptosis in breast cancer cells.

Chemotherapeutic drugs often trigger apoptosis in tumor cells by initiating oxidative stress and generating excessive ROS. Oxidative stress disrupts the equilibrium between oxidizing agents and antioxidants, resulting in an excess of oxidizing substances.[38] The method by which NPs induce toxicity in cancer cells involves the generation of ROS, which results in DNA damage and apoptosis.[39,40] Most of the anticancer drugs available mostly exert their anticancer activity by inducing oxidative stress-mediated cell death.[41] The present findings found that the treatment of MDA-MB-231 cells by the SnO_2-SA-CA HNMs effectively increased the oxidative stress markers and MDA levels, thereby facilitating the oxidative stress.

Oxidative stress arises from an imbalance in the oxidant-antioxidant ratio, resulting in the heightened accumulation of free radicals and consequent damage to biological macromolecules.[42] Cancer cells often accumulate higher levels of anticancer drugs compared to normal cells, indicating that they might possess enhanced protection against the harmful effects of ROS. The fact that antioxidants can protect tumor cells from oxidative stress caused by drugs in an *in vitro* breast cancer model supports the idea that antioxidants may have negative effects on cancer therapy.[43,44] In this work, the findings highlighted that the SnO_2-SA-CA HNMs treatment of the MDA-MB-231 cells resulted in a substantial reduction in the levels of CAT, SOD and GSH. The reduction confirms the onset of oxidative stress and associated apoptosis in the MDA-MB-231 cells.

CONCLUSION

The present study has found that synthesized SnO_2-SA-CA HNMs have a significant effect on inhibiting viability and inducing apoptosis in MDA-MB-231 cells. The SnO_2-SA-CA HNMs have demonstrated substantial effects in inhibiting cell viability, increasing oxidative stress and inducing apoptosis in MDA-MB-231 cells. The findings highlight that SnO_2-SA-CA HNMs exhibit potential as a potential therapeutic candidate to treat breast cancer. Nevertheless, further corroborative studies are needed to thoroughly comprehend the exact molecular mechanisms underlying the anti-cancer mechanisms of SnO_2-SA-CA HNMs against breast cancer.

ACKNOWLEDGEMENT

This project was supported by Researchers Supporting Project number (RSP2024R177) King Saud University, Riyadh, Saudi Arabia.

CONFLICT OF INTEREST

The authors declare that there is no conflict of interest.

ABBREVIATIONS

PL: Photoluminescence; **XRD:** X-ray diffraction; **DLS:** Dynamic light scattering; **SEM:** Scanning electron microscopy; **TEM:** Transmission electron microscopy; **FTIR:** Fourier transform infrared; **DMEM:** Dulbecco's modified Eagle's medium; **FBS:** Fetal bovine serum; **NPs:** Nanoparticles; **CA:** Chlorogenic acid; **SA:** Sodium alginate; **MDA:** Malondialdehyde; **GSH:** Glutathione; **SOD:** Superoxide dismutase; **CAT:** Catalase.

SUMMARY

The present work was focused on synthesizing and characterizing the tin oxide-sodium alginate-chlorogenic acid hybrid nanomaterials (SnO_2-SA-CA HNMs) for enhanced anticancer effects against breast cancer MDA-MB-231 cells. The synthesized SnO_2-SA-CA HNMs were characterized using several methods, including UV-vis spectroscopy, XRD, SEM, EDX, FT-IR, DLS and Photoluminescence (PL) analyses. Also MTT assay, dual staining assay and oxidative stress parameter levels was done to assess the SnO_2-SA-CA HNMs against MDA-MB-231 cells. The results SnO_2-SA-CA HNMs have a crystalline nature, clustered morphology and cuboidal structures. The existence of various functional groups and elements in the HNMs was also confirmed by the FT-IR and DLS analyses, respectively. The SnO_2-SA-CA HNMs have demonstrated substantial effects in inhibiting cell viability, increasing oxidative stress and inducing apoptosis in MDA-MB-231 cells.

REFERENCES

1. Nance E, Pun SH, Saigal R, Sellers DL. Drug delivery to the central nervous system. Nature Reviews Materials. 2022;7(4):314-31.
2. Chivere VT, Kondiah PP, Choonara YE, Pillay V. Nanotechnology-based biopolymeric oral delivery platforms for advanced cancer treatment. Cancers. 2020;12(2):522.
3. Zhang W, Lu Y, Zang Y, Han J, Xiong Q, Xiong J. Photodynamic therapy and multi-modality imaging of up-conversion nanomaterial doped with AuNPs. International Journal of Molecular Sciences. 2022;23(3):1227.
4. Bray F., Ferlay J., Soerjomataram I., Siegel R.L., Torre L.A., Jemal A. Global cancer statistics 2018: GLOBOCAN estimates of incidence and mortality worldwide for 36 cancers in 185 countries. CA Cancer J. Clin. 2018;68:394-424.
5. Wilkinson L, Gathani T. Understanding breast cancer as a global health concern. The British journal of radiology. 2022;95(1130):20211033.
6. Sung H, Ferlay J, Siegel RL, Laversanne M, Soerjomataram I, Jemal A, *et al.* Global cancer statistics 2020: GLOBOCAN estimates of incidence and mortality worldwide for 36 cancers in 185 countries. CA: a cancer journal for clinicians. 2021;71(3):209-49.
7. Arnold M, Morgan E, Rumgay H, Mafra A, Singh D, Laversanne M, *et al.* Current and future burden of breast cancer: Global statistics for 2020 and 2040. The Breast. 2022;66:15-23.
8. Bodewes FT, Van Asselt AA, Dorrius MD, Greuter MJ, De Bock GH. Mammographic breast density and the risk of breast cancer: a systematic review and meta-analysis. The Breast. 2022;66:62-8.
9. Barzaman K, Moradi-Kalbolandi S, Hosseinzadeh A, Kazemi MH, Khorramdelazad H, Safari E, *et al.* Breast cancer immunotherapy: Current and novel approaches. International immunopharmacology. 2021;98:107886.
10. Bukowski K, Kciuk M, Kontek R. Mechanisms of multidrug resistance in cancer chemotherapy. International journal of molecular sciences. 2020;21(9):3233.
11. Alphandéry E. Natural metallic nanoparticles for application in nano-oncology. International Journal of Molecular Sciences. 2020;21(12):4412.
12. Aiello P, Consalvi S, Poce G, Raguzzini A, Toti E, Palmery M, *et al.* Dietary flavonoids: Nano delivery and nanoparticles for cancer therapy. InSeminars in Cancer Biology 2021;150-165.
13. de la Torre P, Pérez-Lorenzo MJ, Alcázar-Garrido Á, Flores AI. Cell-based nanoparticles delivery systems for targeted cancer therapy: lessons from anti-angiogenesis treatments. Molecules. 2020;25(3):715.
14. Lakkakula JR, Gujarathi P, Pansare P, Tripathi S. A comprehensive review on alginate-based delivery systems for the delivery of chemotherapeutic agent: Doxorubicin. Carbohydrate polymers. 2021;259:117696.
15. Dodero A, Alberti S, Gaggero G, Ferretti M, Botter R, Vicini S, Castellano M. An up-to-date review on alginate nanoparticles and nanofibers for biomedical and pharmaceutical applications. Advanced Materials Interfaces. 2021;8(22):2100809.
16. Honarmand M, Golmohammadi M, Naeimi A. Biosynthesis of tin oxide (SnO2) nanoparticles using jujube fruit for photocatalytic degradation of organic dyes. Advanced Powder Technology. 2019;30(8):1551-7.
17. Haq S, Rehman W, Waseem M, Meynen V, Awan SU, Khan AR, *et al.* Effect of Annealing Temperature on Structural Phase Transformations and Band Gap Reduction for Photocatalytic Activity of Mesopores TiO2 Nanocatalysts. Journal of Inorganic and Organometallic Polymers and Materials. 2021;31:1312-22.
18. Miao M, Xiang L. Pharmacological action and potential targets of chlorogenic acid. Advances in pharmacology. 2020;87:71-88.
19. Pimpley V, Patil S, Srinivasan K, Desai N, Murthy PS. The chemistry of chlorogenic acid from green coffee and its role in attenuation of obesity and diabetes. Preparative biochemistry & biotechnology. 2020;50(10):969-78.
20. Yan Y, Zhou X, Guo K, Zhou F, Yang H. Use of chlorogenic acid against diabetes mellitus and its complications. Journal of Immunology Research. 2020; 2020:1-6.
21. Gupta A, Atanasov AG, Li Y, Kumar N, Bishayee A. Chlorogenic acid for cancer prevention and therapy: Current status on efficacy and mechanisms of action. Pharmacol Res. 2022;186:106505.
22. Villota H, Santa-González GA, Uribe D, Henao IC, Arroyave-Ospina JC, Barrera-Causil CJ, Pedroza-Díaz J. Modulatory Effect of Chlorogenic Acid and Coffee Extracts on Wnt/β-Catenin Pathway in Colorectal Cancer Cells. Nutrients. 2022;14(22):4880.
23. Murai T, Matsuda S. The Chemopreventive Effects of Chlorogenic Acids, Phenolic Compounds in Coffee, against Inflammation, Cancer and Neurological Diseases. Molecules. 2023;28(5):2381.
24. Ke Y, Ma Z, Ye H, Guan X, Xiang Z, Xia Y, Shi Q. Chlorogenic Acid-Conjugated Nanoparticles Suppression of Platelet Activation and Disruption to Tumor Vascular Barriers for Enhancing Drug Penetration in Tumor. Adv Healthc Mater. 2023;12(9):e2202205.
25. Curcio M, Diaz-Gomez L, Cirillo G, Nicoletta FP, Leggio A, Iemma F. Dual-targeted hyaluronic acid/albumin micelle-like nanoparticles for the vectorization of doxorubicin. Pharmaceutics. 2021;13(3):304.
26. Hua S., de Matos M.B.C., Metselaar J.M., Storm G. Current Trends and Challenges in the Clinical Translation of Nanoparticulate Nanomedicines: Pathways for Translational Development and Commercialization. Front. Pharmacol. 2018;9:790.
27. Yagawa Y, Tanigawa K, Kobayashi Y, Yamamoto M. Cancer immunity and therapy using hyperthermia with immunotherapy, radiotherapy, chemotherapy and surgery. J. Cancer Metastasis Treat. 2017;3(10):218.
28. Barchiesi G, Mazzotta M, Krasniqi E, Pizzuti L, Marinelli D, Capomolla E, *et al.* Neoadjuvant endocrine therapy in breast cancer: current knowledge and future perspectives. International journal of molecular sciences. 2020;21(10):3528.
29. Gote V, Nookala AR, Bolla PK, Pal D. Drug resistance in metastatic breast cancer: tumor targeted nanomedicine to the rescue. International journal of molecular sciences. 2021;22(9):4673.
30. Yao Y, Zhou Y, Liu L, Xu Y, Chen Q, Wang Y, *et al.* Nanoparticle-based drug delivery in Cancer Therapy and its role in overcoming Drug Resistance. Front Mol Biosci. 2020;1-14.
31. El-Baz AF, El-Enshasy HA, Shetaia YM, Mahrous H, Othman NZ, Yousef AE. Semi-industrial scale production of a new yeast with probiotic traits, Cryptococcus sp. YMHS, isolated from the Red Sea. Probiot Antimicrob Proteins. 2018;10:77-88.
32. Niaz S, Forbes B, Raimi-Abraham BT. Exploiting endocytosis for non-spherical nanoparticle cellular uptake. Nanomanufacturing. 2022;2(1):1-6.
33. Wende M, Sithole S, Chi GF, Stevens MY, Mukanganyama S. The effects of combining cancer drugs with compounds isolated from *Combretum zeyheri* Sond. and *Combretum platypetalum* Welw. ex MA Lawson (Combretaceae) on the viability of Jurkat T cells and HL-60 cells. BioMed Research International. 2021; 2021.
34. Yamaguchi Y, Shiraki K, Fuke H, Inoue T, Miyashita K, Yamanaka Y, *et al.* Targeting of X-linked inhibitor of apoptosis protein or Survivin by short interfering RNAs sensitises hepatoma cells to TNF-related apoptosis-inducing ligand- and chemotherapeutic agent-induced cell death. Oncol Rep. 2005;12:1211-1316.
35. Elmore S. Apoptosis: a review of programmed cell death. Toxicologic pathology. 2007;35(4):495-516.
36. Kroemer G, El-Deiry WS, Golstein P, Peter ME, Vaux D, Vandenabeele P, *et al.* Classification of cell death: recommendations of the Nomenclature Committee on Cell Death. Cell Death Differ. 2005;12:1463-1467.
37. Rizzuto R, Giorgi C, Romagnoli A, Pinton P. Ca2+ signaling, mitochondria and cell death. Current molecular medicine. 2008;8(2):119-30.

38. Ebrahimi S, Hashemy SI. MicroRNA-mediated redox regulation modulates therapy resistance in cancer cells: clinical perspectives. Cellu Oncol. 2019;42:131-141.
39. Bhattacharyya S, Kudgus RA, Bhattacharya R, *et al.* Inorganic nanoparticles in cancer therapy. Pharm Res. 2011;28(2):237-259.
40. Klein S, Sommer A, Distel LV, Hazemann JL, Kröner W, Neuhuber W, *et al.* Superparamagnetic iron oxide nanoparticles as novel X-ray enhancer for low-dose radiation therapy. The Journal of Physical Chemistry B. 2014;118(23):6159-66.
41. Wu H, Wang Y, Ying M. Lactate dehydrogenases amplify reactive oxygen species in cancer cells in response to oxidative stimuli. Signal Transduction Targeted Ther. 2021;6:242.
42. Bansal A, Simon MC. Glutathione metabolism in cancer progression and treatment resistance. J Cell Biol. 2018;217:2291-2298.
43. Ahmed NS, Samec M, Liskova A, Kubatka P, Saso L. Tamoxifen and oxidative stress: an overlooked connection. Discov Oncol. 2021;12:17-31.
44. Zhu Z, Du S, Du Y, Ren J, Ying G, Yan Z. Glutathione reductase mediates drug resistance in glioblastoma cells by regulating redox homeostasis. J neurochem. 2018;144:93-104.

Cite this article: Shakila B, Alyami NM, Aljawdah HM, Alharbi SA, Arulselvan P, Jaganathan SK, *et al*. Chlorogenic Acid Functionalized Tin Oxide-Sodium Alginate Hybrid Nanomaterials Induce Oxidative Stress-Mediated Apoptosis in Breast Cancer MDA-MB-231 Cells. Indian J of Pharmaceutical Education and Research. 2025;59(2):757-66.